


RESEARCH ARTICLE

Open Access



# Identification of a novel DNA oxidative damage repair pathway, requiring the ubiquitination of the histone variant macroH2A1.1

Khalid Ouararhni<sup>1†</sup>, Flore Mietton<sup>2†</sup>, Jamal S. M. Sabir<sup>3,4†</sup>, Abdulkhaleg Ibrahim<sup>1,5</sup>, Annie Molla<sup>2</sup>, Raed S. Albheyri<sup>3,4</sup>, Ali T. Zari<sup>3,4</sup>, Ahmed Bahieldin<sup>3,4</sup>, Hervé Menoni<sup>2</sup>, Christian Bronner<sup>1</sup>, Stefan Dimitrov<sup>2,6\*</sup> and Ali Hamiche<sup>1\*</sup> 

## Abstract

**Background** The histone variant macroH2A (mH2A), the most deviant variant, is about threefold larger than the conventional histone H2A and consists of a histone H2A-like domain fused to a large Non-Histone Region responsible for recruiting PARP-1 to chromatin. The available data suggest that the histone variant mH2A participates in the regulation of transcription, maintenance of heterochromatin, NAD<sup>+</sup> metabolism, and double-strand DNA repair.

**Results** Here, we describe a novel function of mH2A, namely its implication in DNA oxidative damage repair through PARP-1. The depletion of mH2A affected both repair and cell survival after the induction of oxidative lesions in DNA. PARP-1 formed a specific complex with mH2A nucleosomes *in vivo*. The mH2A nucleosome-associated PARP-1 is inactive. Upon oxidative damage, mH2A is ubiquitinated, PARP-1 is released from the mH2A nucleosomal complex, and is activated. The *in vivo*-induced ubiquitination of mH2A, in the absence of any oxidative damage, was sufficient for the release of PARP-1. However, no release of PARP-1 was observed upon treatment of the cells with either the DNA alkylating agent MMS or doxorubicin.

**Conclusions** Our data identify a novel pathway for the repair of DNA oxidative lesions, requiring the ubiquitination of mH2A for the release of PARP-1 from chromatin and its activation.

**Keywords** Histone variant, mH2A, PARP-1, DNA repair, Chromatin

<sup>†</sup>Khalid Ouararhni, Flore Mietton and Jamal S. M. Sabir contributed equally to this work.

\*Correspondence:  
Stefan Dimitrov  
stefan.dimitrov@univ-grenoble-alpes.fr  
Ali Hamiche  
hamiche@igbmc.fr

<sup>1</sup> Département de Génomique Fonctionnelle Et Cancer, Institut de Génétique Et Biologie Moléculaire Et Cellulaire (IGBMC), Université de Strasbourg/CNRS/INSERM, Equipe Labellisée La Ligue Nationale Contre Le Cancer, 67404 Illkirch Cedex, France

<sup>2</sup> Institute for Advanced Biosciences, Inserm U 1209, CNRS UMR 5309, Université Grenoble Alpes, 38000 Grenoble, France

<sup>3</sup> Centre of Excellence in Bionanoscience Research, King Abdulaziz University, Jeddah, Saudi Arabia

<sup>4</sup> Department of Biological Sciences, Faculty of Science, King Abdulaziz University, Jeddah, Saudi Arabia

<sup>5</sup> National Research Centre for Tropical and Transboundary Diseases (NRCTTD), Alzentan 99316, Libya

<sup>6</sup> Institute of Molecular Biology Roumen Tsanev, Bulgarian Academy of Sciences, Sofia, Bulgaria



## Background

In addition to conventional core histones, eukaryotic cells express histone variants [1]. Histone variants are nonallelic histone isoforms, which can substitute for the respective conventional histone. Histone variants are deposited into chromatin by the help of dedicated histone variant chaperone complexes [2–5] and their incorporation into the nucleosome can affect both its structural and functional properties [6–10]. For example, specific structural features of the histone variant nucleosomes could interfere with the ability of chromatin remodeling machines to remodel and mobilize them [11–14] or to allow the recognition and interaction with distinct proteins [15, 16].

All conventional histones, except H4, possess histone variants. Histone H2A has the largest number of histone variants [17]. Histone macroH2A (mH2A), the most deviant histone variant, is about three fold larger than the conventional H2A and consists of a histone H2A-like domain fused to a large Non-Histone Region (NHR) [18]. Two mH2A genes, mH2A1 and mH2A2, were identified in humans [19, 20]. In turn, mH2A1 has two splice variants, mH2A1.1 and mH2A1.2 [19].

Diverse functions were attributed to mH2A, including transcriptional repression, heterochromatin organization, Nicotinamide adenine dinucleotide (NAD<sup>+</sup>) MMS-metabolism and DNA repair (for recent reviews see [21, 22]). Studies with reconstituted mH2A nucleosomes and nucleosomal arrays have suggested that mH2A is implicated in the control of gene expression [6]. These *in vitro* data were supported by *in vivo* experiments [23, 24]. Immunofluorescence data suggested that the inactive X chromosome (Xi) was enriched in mH2A since a more pronounced staining with mH2A antibody of the Xi chromosome compared to other nucleus regions was observed [25]. At least part of this staining could be attributed to the higher nucleosome density characteristic of the condensed Xi chromosome and not to enrichment with mH2A [26]. In agreement, mH2A was found depleted from the transcribed regions of active genes in mouse liver [27]. It was also reported that mH2A took part in the inhibition of both Mesenchymal-to-Epithelial and Epithelial-to-Mesenchymal Transitions [28, 29]. One of the spliced variants of macroH2A.1, macroH2A1.2, is involved in telomere organization and function [30]. Mitochondrial respiration appeared to be controlled by macroH2A.1.1 via limitation of nuclear NAD<sup>+</sup> consumption [31]. Implication of macroH2A in double-strand-break repair was also reported [32]. PARP1-dependent chromatin relaxation, that occurs in living cells upon DNA damage, was also described [33].

In cells, oxidative stress can be induced by an increased level of hydrogen peroxide (H<sub>2</sub>O<sub>2</sub>), which could lead to

cellular damage. The increased level of H<sub>2</sub>O<sub>2</sub> generates single strand breaks (SSB) in DNA, either directly or indirectly (mainly by the cleavage of the oxidized guanine lesion, 8-oxoguanine [34]).

Poly(ADP-ribose) polymerase I (PARP-1) is a molecular sensor of DNA breaks and it is intimately related to their repair (for recent reviews see [35]). The enzyme uses NAD<sup>+</sup> for the synthesis and attachment of the poly(ADP-ribose) polymer (PAR) to its substrates, which among others include histones, SSB repair proteins and PARP-1 itself. The poly(ADP-ribosylation) of histone H1 was shown to perturb its interaction with chromatin, which resulted in a decondensation of the 30 nm chromatin fiber and allowed the repair complexes to assemble at the damaged site [35–37]. The poly(ADP-ribose) glycohydrolase (NAD) hydrolyzes the glycosidic bond between the ADP-ribose units and thus, generates free ADP-ribose [35]. The elimination of PAR creates conditions for condensation of the repaired chromatin fiber.

In this work, we present direct evidence for a novel function of mH2A, namely its involvement in DNA oxidative damage repair. *In vivo* PARP-1 forms a stable complex with mH2A chromatin. Upon generation of oxidative DNA lesions mH2A is ubiquitinated. As a result, PARP-1 is released from the ubiquitinated mH2A chromatin and activated. The ubiquitination of mH2A alone is sufficient for the release of PARP-1 from chromatin. These data identify a novel pathway for the repair of oxidative DNA lesions, which requires the ubiquitination of mH2A.

## Results

### mH2A1 is involved in DNA oxidative damage repair

To study the potential involvement of mH2A1 in DNA repair, we used HeLa cells where mH2A1 levels were reduced by siRNA. The suppression of the mH2A1 expression was confirmed by a specially generated anti-mH2A1 antibody [26]. Transfection of HeLa cells with siRNA resulted in a very efficient suppression (more than 80%) of the expression of mH2A1 (Fig. 1B). The control cells, the knock down and rescue cells (expressing an siRNA resistant mH2A1.1, see methods) were then subjected to oxidative damage by treatment with 10 mM H<sub>2</sub>O<sub>2</sub> for 5 minutes, and the cells allowed to recover for the indicated times ranging from 5 minutes to 1 hour. The presence of single-strand breaks (SSB) in the H<sub>2</sub>O<sub>2</sub> treated cells was studied by a Comet assay under alkaline conditions (Fig. 1A-C). The Comet assay showed the presence of a higher amount of residual SSB in the mH2A1 siRNA transfected cells relative to that of the control or rescue cells at the corresponding time points (Fig. 1A, compare, for example, the 5 and 15 minutes time points for control and siRNA treated cells). The quantification

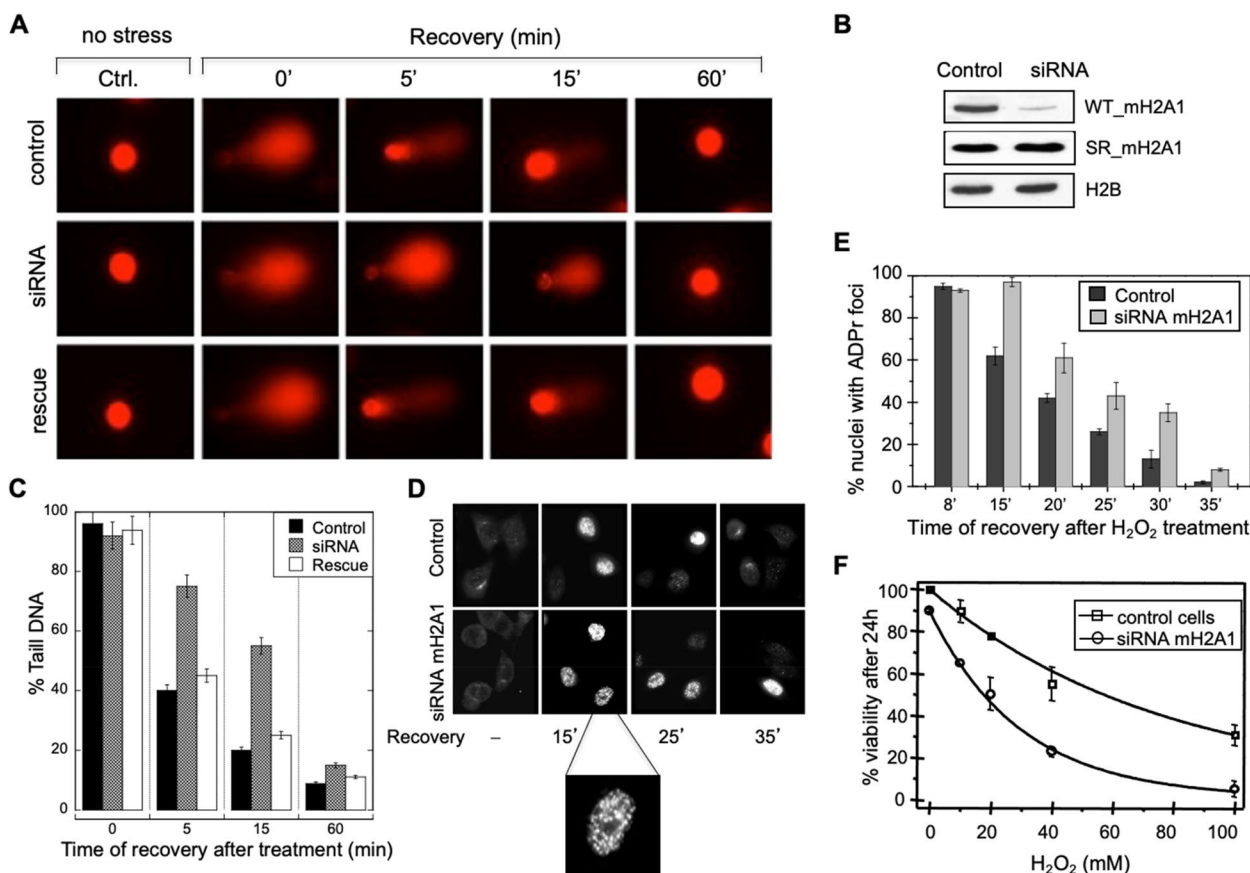


**Fig. 1** The presence of mH2A is essential for the repair of DNA damage and cell survival upon treatment with H<sub>2</sub>O<sub>2</sub>. **A** Control (transfected with scrambled siRNA), siRNA resistant (SR) and siRNA mH2A1 transfected cells were treated with H<sub>2</sub>O<sub>2</sub>, allowed to recover for the indicated times, and were then subjected to alkaline Comet assay. **B** Western blot analysis of total cell extract prepared from control and mH2A1 siRNA transfected cells. The blot was first probed with anti-mH2A1 and then with an anti-H2B antibody as a control for equal protein loading. **C** Quantification of the Comet assay data. Values represent means and standard deviations for ~ 300 cells from 3 independent experiments. **D** The removal of nuclear poly-ADP ribose foci induced after oxidative DNA damage is dependent on the presence of mH2A1. Control and mH2A1 siRNA transfected HeLa cells were treated with H<sub>2</sub>O<sub>2</sub>, allowed to recover for the indicated times and then fixed and immunostained with anti-poly(ADP-ribose) antibody. **E** Quantification of the data presented in (D). The means of two independent experiments are presented. For each time point no less than 100 cells were analyzed. **F** mH2A1 is required for cell survival after oxidative stress. Control and mH2A1 siRNA transfected HeLa cells were treated with H<sub>2</sub>O<sub>2</sub> at the indicated concentrations. The percentage cell survival was measured 24 h after the H<sub>2</sub>O<sub>2</sub> treatment. The means of 3 different experiments are shown

of the Comet assay data demonstrated slower SSB repair kinetics in mH2A1 depleted cells. Indeed, the rate of the disappearance of the tail DNA (Fig. 1C) was about five to seven-fold slower in the mH2A1 depleted cells compared to the control or rescue cells. We conclude that the suppression of mH2A1 expression affected SSB repair, providing thus evidence that mH2A1 was required for this process.

To further test this hypothesis, we have carried out immunofluorescence experiments by using anti-poly-ADP-ribose (anti-PAR) antibodies to visualize the PAR foci in H<sub>2</sub>O<sub>2</sub> treated cells. The PAR foci are generated by PARP-1 ribosylation of specific proteins in vicinity of

the damaged sites. The presence of the PAR foci is evidence for active repair process (for a review see [35]). Once the DNA damage is repaired, the PAR is degraded by the glycohydrolase PARG and the foci are, thus, removed [35, 38]. PAR foci were present after DNA damage in both control and mH2A1 depleted cells (Fig. 1D), but the number of cells presenting such foci decreased more slowly in the mH2A1 knocked down cells (Fig. 1E). These data illustrate the requirement of mH2A for efficient repair of the oxidatively damaged DNA and are in full agreement with the Comet assay results described above (Fig. 1A-C). Therefore, we have shown by two independent approaches the involvement of mH2A in the repair of DNA after oxidative damage.

If mH2A1 was required for DNA repair, one would expect the suppression of mH2A1 expression to also affect the viability of H<sub>2</sub>O<sub>2</sub> treated cells. To test this idea, we treated both control and mH2A1 depleted cells with different concentrations of H<sub>2</sub>O<sub>2</sub>, and measured cell viability 24 hours post treatment. It is clear from the data (Fig. 1F) that the absence of mH2A1 interfered with cell survival. Indeed, upon H<sub>2</sub>O<sub>2</sub> treatment the viability of the cells transfected with the mH2A1 siRNA was decreased compared to the control cells. For example, the treatment with 40 mM H<sub>2</sub>O<sub>2</sub> reduced the survival of the mH2A1 depleted cells more than two-fold i.e. from about 50% in control cells to about 20% in the mH2A1-knocked down cells (Fig. 1F).

**Treatment of cells with H<sub>2</sub>O<sub>2</sub> results in the release of PARP-1 from mH2A chromatin and its activation**

W and others have previously demonstrated that PARP-1 is specifically associated with mH2A nucleosomes into

the cell [24, 39]. Importantly, the *in vivo* association of PARP-1 with mH2A chromatin downregulated its enzymatic activity [24]. GST-pull down experiments have shown that the association of PARP-1 with mH2A nucleosomes was achieved through the NHR of mH2A1 [24, 39]. In addition, enzymatic assays demonstrated that the NHR of mH2A inhibited PARP-1 enzymatic activity *in vitro* [39]. Taken together, these data suggest that *in vivo* mH2A could act as a negative regulator of PARP-1 enzymatic activity, which, in turn, indicates that mH2A could be involved in the DNA damage repair through PARP-1. We hypothesized that the dissociation of PARP-1 from mH2A chromatin upon H<sub>2</sub>O<sub>2</sub> cell treatment could activate PARP-1 and facilitate its recruitment to the DNA lesions. We have addressed this possibility by using a HeLa cell line stably expressing epitope-tagged mH2A1.1 (Fig. 2 and [24]). It is important to note that the expression level of the tagged protein did not exceed 40% of the endogenous mH2A1 (Fig. 2B). These cells were treated

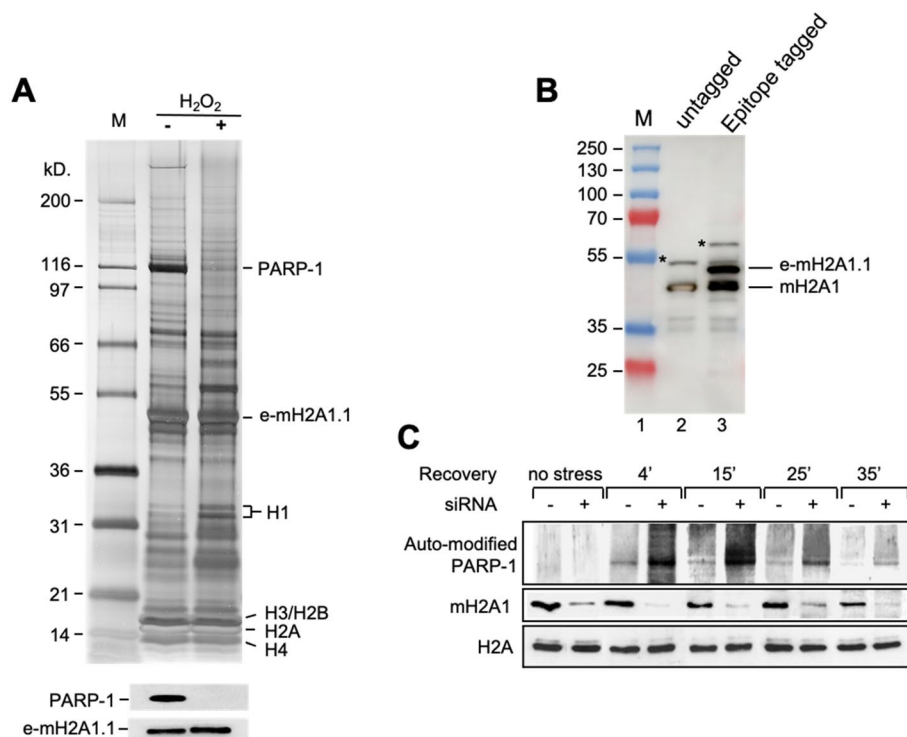


**Fig. 2** Upon H<sub>2</sub>O<sub>2</sub> treatment, mH2A1.1 is ubiquitinated and PARP-1 is both released from the e-mH2A1.1 nucleosome complex and activated. **A** Silver staining e-mH2A1.1 nucleosome complex (run on SDS PAGE) isolated from either control (-) or H<sub>2</sub>O<sub>2</sub> (+) treated HeLa cells stably expressing e-mH2A1.1. The proteins identified by mass spectrometry are indicated. Lane M, molecular mass markers. The masses of the different protein markers are indicated. The lower part of the Figure shows the Western blot of e-mH2A1.1 nucleosomal complexes isolated from control (-) and H<sub>2</sub>O<sub>2</sub> (+) treated e-mH2A1.1 stable HeLa cell lines. The blot was first probed with anti-PARP-1 antibody and then, to visualize e-mH2A1.1, it was probed with anti-HA antibody. **B** Western blot quantification of mH2A1.1 expression level in untagged and epitope tagged HeLa cells. \* indicates the ubiquitinated form of mH2A1. **C** Kinetics of PARP-1 auto-ADP-ribosylation after oxidative DNA damage in control and mH2A1 siRNA transfected HeLa cells. Cells were treated with H<sub>2</sub>O<sub>2</sub> and after recovery for the indicated times, the cell lysates were run on SDS PAGE, transferred and the blots were probed with either anti-poly(ADP-ribose) antibody (upper panel) or with anti-macroH2A1 (middle panel) or anti-H2A antibodies (lower panel), respectively

with H<sub>2</sub>O<sub>2</sub>, and epitope-tagged mH2A1.1 (e-mH2A1.1) nucleosomal complexes were immunopurified from treated and control cells as described [24]. In agreement with our earlier observations [24], we identified PARP-1 within the e-mH2A1.1 nucleosomal complex isolated from non-treated control cells (Fig. 2A, upper and lower panels). Remarkably, treatment with H<sub>2</sub>O<sub>2</sub> resulted in release of PARP-1 from e-mH2A1.1 nucleosomal complexes as demonstrated by both electrophoretic and Western blot analyses (Fig. 2A).

We next asked if the PARP-1 released from the mH2A nucleosomal complex was more readily activated upon cell treatment with H<sub>2</sub>O<sub>2</sub>. To generate “released from mH2A chromatin” PARP-1 we knocked down the expression of mH2A1 in HeLa cells. Then, we studied the auto-ribosylated status of PARP-1 (which is a strong indication for the presence of activated PARP-1 [37, 40]) in control and H<sub>2</sub>O<sub>2</sub> treated cells. The experiments were carried out as follows. Whole cell extracts were isolated from either control (transfected with scrambled siRNA) or mH2A1 siRNA transfected HeLa cells (after treatment of the cells with H<sub>2</sub>O<sub>2</sub> and subsequent 4, 15, 25 and 35 minutes recovery). Identical aliquots of the extracts were run on an SDS-PAGE (Sodium dodecyl sulfate Polyacrylamide gel), the proteins were transferred, and the blot was probed either with anti-ADP-ribose antibody (Fig. 2C, upper panel; this antibody detects the activated ADP-ribosylated forms of PARP-1 [41]), or with anti-mH2A1 antibody (Fig. 2C, middle panel) or for illustration of the equal loading with anti-H2A antibody (Fig. 2C, lower panel). As seen, at all recovery time points following damage, the amount of auto-modified enzyme in the control cells was always much smaller than that of the mH2A1 siRNA transfected cells (Fig. 2C upper panel, compare the intensities of the bands in the siRNA treated and control cells at the different time points). Interestingly, the bands corresponding to the auto-modified PARP-1 in the mH2A1 knock-down cells were not only higher in intensity, but were also present for longer times (Fig. 2C, see 25 and 35 minutes recovery). We conclude that, following oxidative damage, the siRNA knock-down of mH2A1 led, as expected, to both large increase in the amount of activated PARP-1 and long-lived activated enzyme. Note that these results are in full agreement with the slower kinetics of disappearance of the PAR foci (indicators of active repair process and thus, of active PARP-1) after oxidative damage in mH2A1 knocked down cells compared to these of control cells (Fig. 1D, E).

Intriguingly, the release of PARP-1 from e-mH2A1.1 chromatin was induced specifically by the treatment of the cells with H<sub>2</sub>O<sub>2</sub>, but not with other DNA damaging agents (Additional file 1: Fig. S1). Indeed, as judged by SDS PAGE and Western blotting of the mH2A1.1

nucleosomal complexes isolated from either MMS (Methyl methanesulfonate) or doxorubicin treated cells, no dissociation of PARP-1 was observed, in contrast to H<sub>2</sub>O<sub>2</sub> treated cells (Additional file 1: Fig. S1). In addition, the H<sub>2</sub>O<sub>2</sub> induced dissociation of PARP-1 did not reflect a direct effect of H<sub>2</sub>O<sub>2</sub> on the mH2A1.1 nucleosome complexes, since treatment of isolated e-mH2A1.1 nucleosome complexes with any of the damaging agents did not result in detectable perturbations in the interactions between the partners of the complexes and subsequent release of PARP-1 (Additional file 2: Fig. S2).

### Treatment of cells with H<sub>2</sub>O<sub>2</sub> induces ubiquitination of mH2A.1

As shown above, upon treatment with H<sub>2</sub>O<sub>2</sub> PARP-1 is released from the mH2A1 nucleosomal complex. A possible reason for this release of PARP-1 would be the induction of some perturbations or modifications in the structure of mH2A1 resulting from the H<sub>2</sub>O<sub>2</sub> treatment. We have approached this question by studying the modifications in mH2A1 generated after H<sub>2</sub>O<sub>2</sub> oxidative damage (Fig. 3A). e-mH2A1.1 HeLa cell lines were treated with H<sub>2</sub>O<sub>2</sub> and, after allowing the cells to recover for selected time points, the e-mH2A1.1 complex was isolated and subjected to SDS PAGE (Fig. 3A). Mass spectrometry analysis showed some weak mono-ubiquitination of mH2A1.1 in the control complex (Fig. 3A). Treatment with H<sub>2</sub>O<sub>2</sub> led to a drastic increase of the amount of monoubiquitinated e-mH2A1.1 (e-mH2A1.1-ub1) and the appearance of bi-ubiquitinated e-mH2A1.1 (e-mH2A1.1-ub2). Mass spectrometry analysis identifies lysines 115 and 120 as the first and second sites of ubiquitination (Fig. 3C). Immunoprecipitation of the H<sub>2</sub>O<sub>2</sub>-treated e-mH2A1.1 complex with the anti-ubiquitin FK2 antibody, followed by anti-FLAG antibody blotting, confirmed the ubiquitination of e-mH2A1.1 (Fig. 3D). Note that the amount of mono-ubiquitinated e-mH2A1.1 remained relatively unchanged during the recovery period, while that of bi-ubiquitinated e-mH2A1.1 showed some increase with the time of recovery (Fig. 3A, compare 5 minutes with 30 minutes recovery points). This was further confirmed by Western blotting (Fig. 3B). In contrast, the amount of PARP-1 associated with the e-mH2A1.1 complex sharply dropped after 5 minutes and then gradually decreased (Fig. 3A, B), i.e. the time-course of PARP-1 release was concomitant with this of e-mH2A1.1 ubiquitination.

The control e-mH2A1.1 nucleosomal complex contained small amount of histone H1, but already after 5 minutes of recovery, a full complement of histone H1 was found associated with the e-mH2A1.1 nucleosomal complex (Fig. 3A). The time-course of H1 association with e-mH2A1.1 nucleosome paralleled both those of

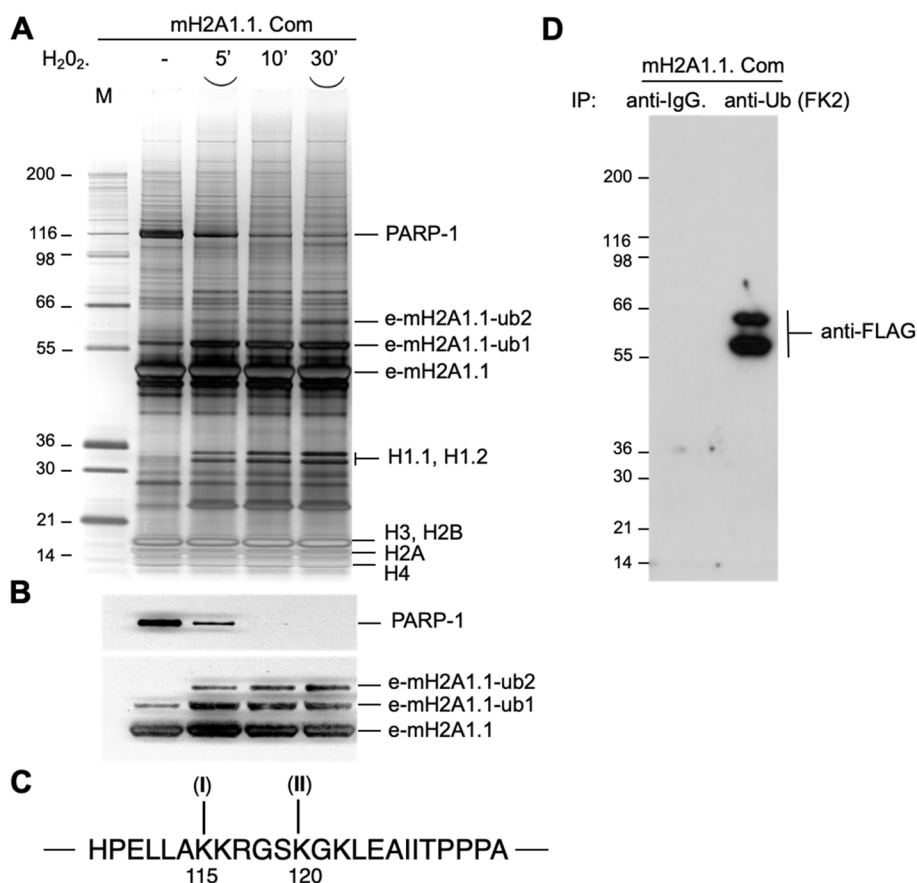


**Fig. 3** mH2A is ubiquitinated upon oxidative stress. **A** Stable HeLa cell lines expressing e-mH2A1.1 were treated with H<sub>2</sub>O<sub>2</sub> and allowed recovering for the times indicated. The e-mH2A1.1 nucleosomal complex was immunopurified, run on a gel containing SDS and proteins were identified by mass spectrometry. The positions of PARP-1, non-modified and mono(ub1)- and bi-ubiquitinated(ub2) e-mH2A1.1, histone H1 and core histones are indicated. **B** Western blot of the e-mH2A1.1 complex. The blot was first revealed with anti-PARP-1 antibody and then with anti-HA antibody for visualization of mH2A1.1. **C** Amino acid sequence of mH2A1.1 encompassing AA 109–132. The positions of the two identified by mass spectrometry ubiquitination sites (I) and (II), corresponding to lysine residues 115 and 120, are indicated. **D** Western blot analysis of the e-mH2A1.1 complex immunoprecipitated either with anti-IgG or with anti-ubiquitin FK2, and blotted with an anti-FLAG antibody

ubiquitination of e-mH2A1.1 and release of PARP-1 from the e-mH2A1.1 nucleosome.

**Mutations of the mH2A ubiquitination sites affects the association with PARP-1**

The e-mH2A1 oxidative-stress dependent ubiquitination and the concomitant release of PARP-1 from the e-mH2A1.1 nucleosomal complex suggest a causal relationship between these two events. We have tested this hypothesis by establishing stable HeLa cell lines, expressing mutated e-mH2A1.1, in which the ubiquitinable lysines 115 and 116 were substituted with alanines (Fig. 4 A).

Then we treated these cells with H<sub>2</sub>O<sub>2</sub> under identical conditions as these of the wild type cells, allowed recovery for 5 minutes and isolated the mutated e-mH2A1.1 nucleosomal complexes. We found that the mutated e-mH2A1.1 was ubiquitinated as much as the wild-type

e-mH2A1.1 nucleosomal complex and that the majority of PARP-1 was released from the mutated e-mH2A1.1 nucleosome (Fig. 4A). Since ubiquitination does not require a specific peptide sequence, this indicated that the mutant e-mH2A1.1 could be ubiquitinated at new sites located in the vicinity of lysines 115 and 116. Analysis of the primary mH2A1.1 sequence in the vicinity of these lysine residues identified two other lysine residues (120 and 122) as potential new sites of ubiquitination. With this in mind, we next established HeLa stable cell lines where either the three lysines 115, 116 and 120 (K115/116/120A) or all the four lysines 115, 116, 120 and 122 (K115/116/120/122A) of e-mH2A1.1 were substituted with alanines. These cell lines were subjected to treatment with H<sub>2</sub>O<sub>2</sub>, allowed to recover and the e-mH2A1.1 mutant nucleosome complexes were purified (Fig. 4A, lanes 5-8). Upon treatment with H<sub>2</sub>O<sub>2</sub>, the ubiquitination of e-mH2A1.1 was strongly decreased only in

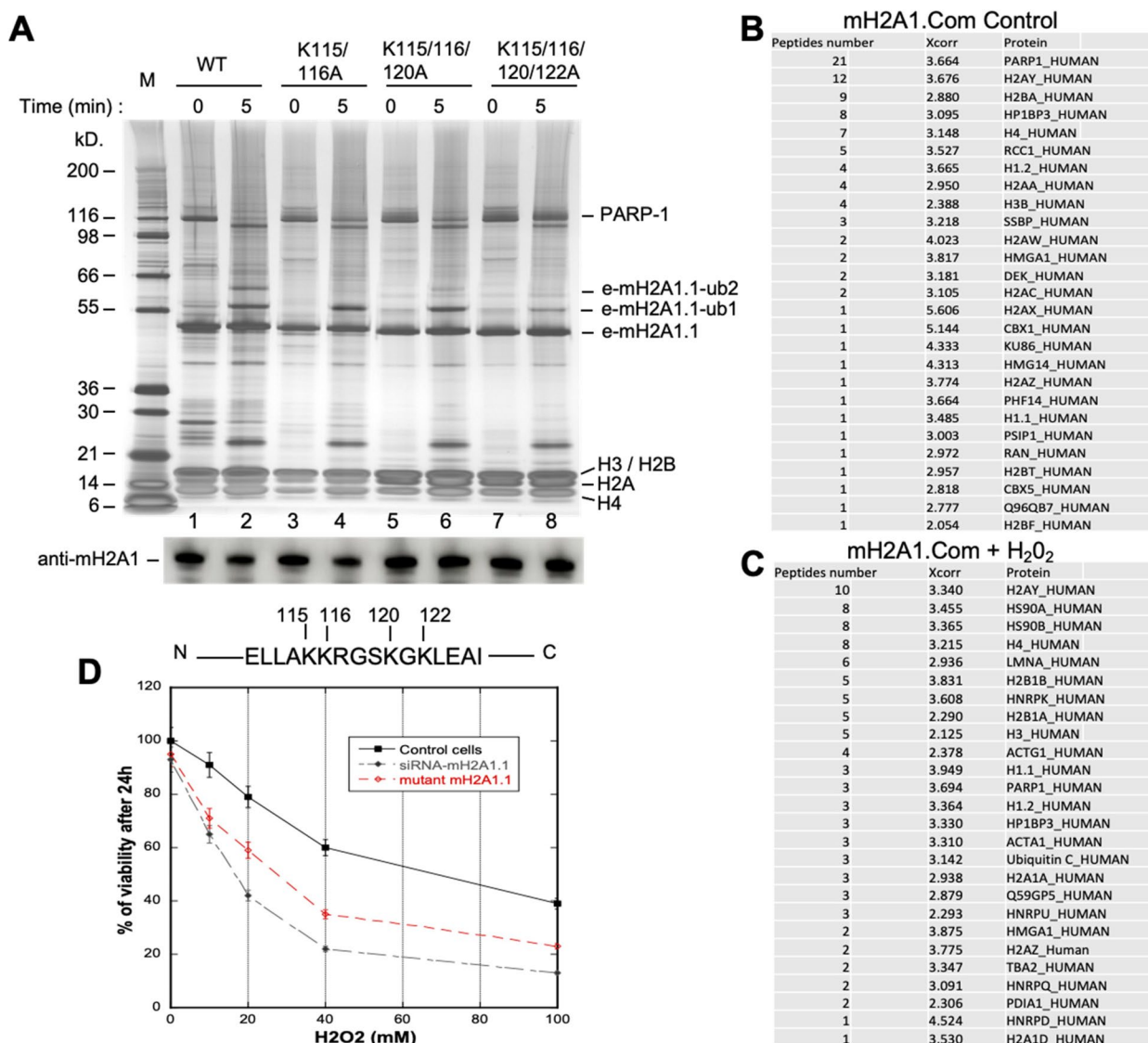


**Fig. 4** The release of PARP-1 from the mH2A1 nucleosomal complex is affected by mutations of the mH2A ubiquitination sites. Stable HeLa cell lines expressing e-mH2A1.1 bearing lysine (K) to alanine (A) mutations either at positions 115 and 116, or at 115, 116 and 120 or at 115, 116, 120 and 122, were established. They were treated with H<sub>2</sub>O<sub>2</sub> and allowed recovering for 5 min (at time point zero (0)), the cells were treated with H<sub>2</sub>O<sub>2</sub> and not allowed to recover). Then the e-mH2A1.1 mutated nucleosome complexes were isolated, run on a SDS PAGE and the proteins and e-mH2A1.1 ubiquitinated species were identified by mass spectrometry. The positions of the identified proteins were indicated at the right part of the figure. M, protein molecular mass markers. The molecular weights of the markers are indicated. In the middle of the figure is shown a Western blot against mH2A1. In the lower part of the figure is shown the amino acid sequence of mH2A1.1 encompassing AA 112–124. The positions of the lysines, which were mutated to alanines, are indicated. (The percentage cell survival was measured 24 h after the H<sub>2</sub>O<sub>2</sub> treatment. The means of 3 different experiments are shown. **B** Mass spectrometry table of the e-mH2A1.1 complex purified from untreated HeLa cells. **C** Mass spectrometry table of the e-mH2A1.1 complex purified from H<sub>2</sub>O<sub>2</sub> treated HeLa cells. **D** Control HeLa cells, mH2A1 siRNA transfected HeLa cells and e-mH2A1.1 K115/116/120/122A mutant HeLa cells were treated with H<sub>2</sub>O<sub>2</sub> at the indicated concentrations

the cell line expressing the emH2A1.1 bearing the four lysine to alanine mutations (Fig. 4A, Lanes 7, 8). Note that a very weak release of PARP-1 from the mutated e-mH2A1.1 chromatin was observed (Fig. 4A, compare lane 7 with lane 8). The above data provide evidence for a mH2A ubiquitination dependent release of PARP-1 from

mH2A chromatin following treatment of cells with H<sub>2</sub>O<sub>2</sub>. The release of PARP-1 from mH2A1.1 was further confirmed by mass spectrometry analysis (Fig. 4B, C).

We then examined how mutations in mH2A1.1 ubiquitination affect the viability of H<sub>2</sub>O<sub>2</sub>-treated cells. To achieve this, we treated control cells, mH2A1 siRNA-depleted

cells, and e-mH2A1.1 K115/116/120/122A mutant HeLa cells with varying concentrations of H<sub>2</sub>O<sub>2</sub> and assessed cell viability 24 hours post-treatment. The data (Fig. 4D) clearly indicate that the mH2A1.1 ubiquitination mutant impairs cell survival in a manner similar to the absence of mH2A1. Indeed, following H<sub>2</sub>O<sub>2</sub> treatment, the viability of mH2A1.1 ubiquitination mutant cells decreased compared to control cells (Fig. 4D).

To further confirm this observation, we have studied the time course of e-mH2A1.1 ubiquitination and have quantified PARP-1 release from chromatin after H<sub>2</sub>O<sub>2</sub> treatment of cell lines expressing either wild type mH2A1.1 or K115/116/120/122A mH2A1.1 mutant (Fig. 5). Intriguingly, before treatment with H<sub>2</sub>O<sub>2</sub> the normalized amount of PARP-1 associated with the e-mH2A1.1 nucleosomes (the ratio PARP-1: e-mH2A1.1 nucleosome) purified from the mutated (K115/116/120/122A) cell line was found to be more than four-fold higher compared to the WT e-mH2A1.1 complex (Fig. 5A, B).

Treatment with H<sub>2</sub>O<sub>2</sub> resulted in a rapid e-mH2A1.1 ubiquitination and a parallel massive release of PARP-1 from the control e-mH2A1.1 nucleosomes (Fig. 5). Already at 10 minutes more than 80% of the nucleosome

associated PARP-1 was released (Fig. 5B). At 30 minutes recovery, a very faint amount (no more than 5%) of PARP-1 remained associated with e-mH2A1.1 in WT cells. In contrast, the release of PARP-1 from the mutated (K115/116/120/122A) e-mH2A1.1 nucleosome was very slow and even at the latest recovery time point (30 minutes) a substantial amount of PARP-1 remained associated with the nucleosome (Fig. 5A, B). Importantly, the normalized amount of PARP-1 associated with the mutated e-mH2A1.1 nucleosome was more than 50-fold higher compared to this associated with the WT e-mH2A1.1 at 30 minutes of recovery (Fig. 5B). We note that in both cases the release of PARP-1 from chromatin is accompanied by a concomitant association of histone H1 with the e-mH2A1.1 complex (Fig. 5A).

**The ubiquitination of mH2A alone is sufficient for quantitative release of PARP-1 from mH2A chromatin**

All the above presented results strongly suggest, but do not directly demonstrate that the release of PARP-1 from chromatin upon H<sub>2</sub>O<sub>2</sub> treatment is a consequence of the ubiquitination of mH2A. To show this, we have treated stable HeLa cells expressing WT e-mH2A1.1

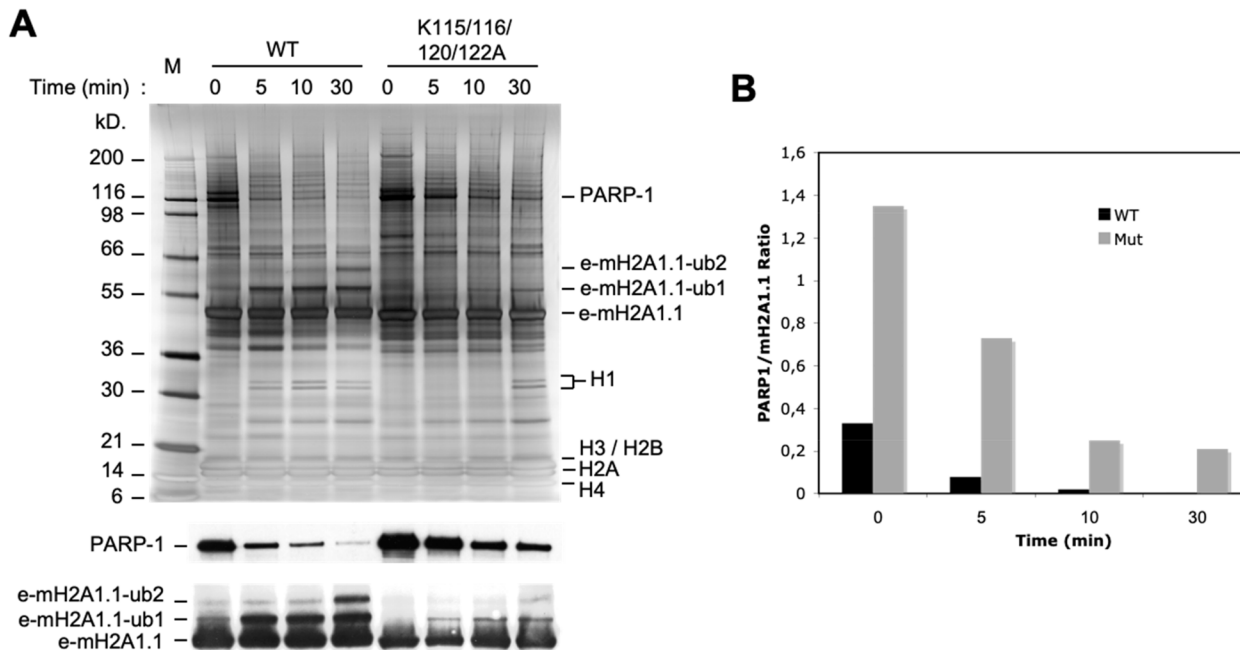


**Fig. 5** Time course of PARP-1 release from mH2A chromatin, induced after treatment with H<sub>2</sub>O<sub>2</sub>. Stable cell lines expressing either wild type mH2A1.1 or four lysine to alanine mutated (K115/116/120/122A) mH2A1.1 were treated with H<sub>2</sub>O<sub>2</sub> and allowed recovering for the times indicated. The mH2A1.1 complexes were then purified, run on SDS PAGE and the proteins were identified by mass spectrometry. The positions of the identified proteins are indicated. The lower part of the figure shows the Western blot analysis of respective e-mH2A1.1 nucleosome complexes. The blot was first probed with anti-PARP-1 antibody and then, to visualize e-mH2A1.1, it was probed with anti-HA antibody. **B** Quantification of the Western blot data shown in **(A)**. The PARP-1/mH2A1.1 ratio for both WT (black) and mutated (grey) mH2A1.1 nucleosomal complexes is presented



with 5 mM NEM (N-ethylmaleimide, a general inhibitor of de-ubiquitination) and have purified the e-mH2A1.1 complex. Both the electrophoretic and the Western blot analyses show that treatment with NEM resulted, as expected, in a massive ubiquitination of e-mH2A1.1 (Fig. 6A). Remarkably, in the absence of H<sub>2</sub>O<sub>2</sub> treatment PARP-1 was completely released from the ubiquitinated, but not from the non-modified e-mH2A1.1 nucleosome complex (Fig. 6A). Again, the release of PARP-1 was paralleled with association of histone H1 with the ubiquitinated e-mH2A1.1 nucleosomes. Therefore, the *in vivo* ubiquitinated mH2A nucleosome complexes are not associated with PARP-1 further showing that ubiquitination of mH2A is sufficient for the release of PARP-1 from the mH2A chromatin.

### Discussion

In this work, we demonstrate a novel function of mH2A1, namely its direct involvement in DNA oxidative damage repair. The repair of oxidative DNA damage was compromised in cells with siRNA suppressed expression of mH2A1, and the survival of these cells after the damage was also affected. To decipher the mechanism of involvement of mH2A1 in DNA repair we have analyzed the partners associated with mH2A1 nucleosomes *in vivo*. In agreement with earlier data [24], we found that PARP-1 was associated with mH2A.1 nucleosomes. Treatment with the DNA oxidative damaging agent H<sub>2</sub>O<sub>2</sub> resulted in release of the mH2A1 associated PARP-1. The mH2A1 immobilized PARP-1 was inactive and the depletion of mH2A1 resulted, upon induction of oxidative damage, in

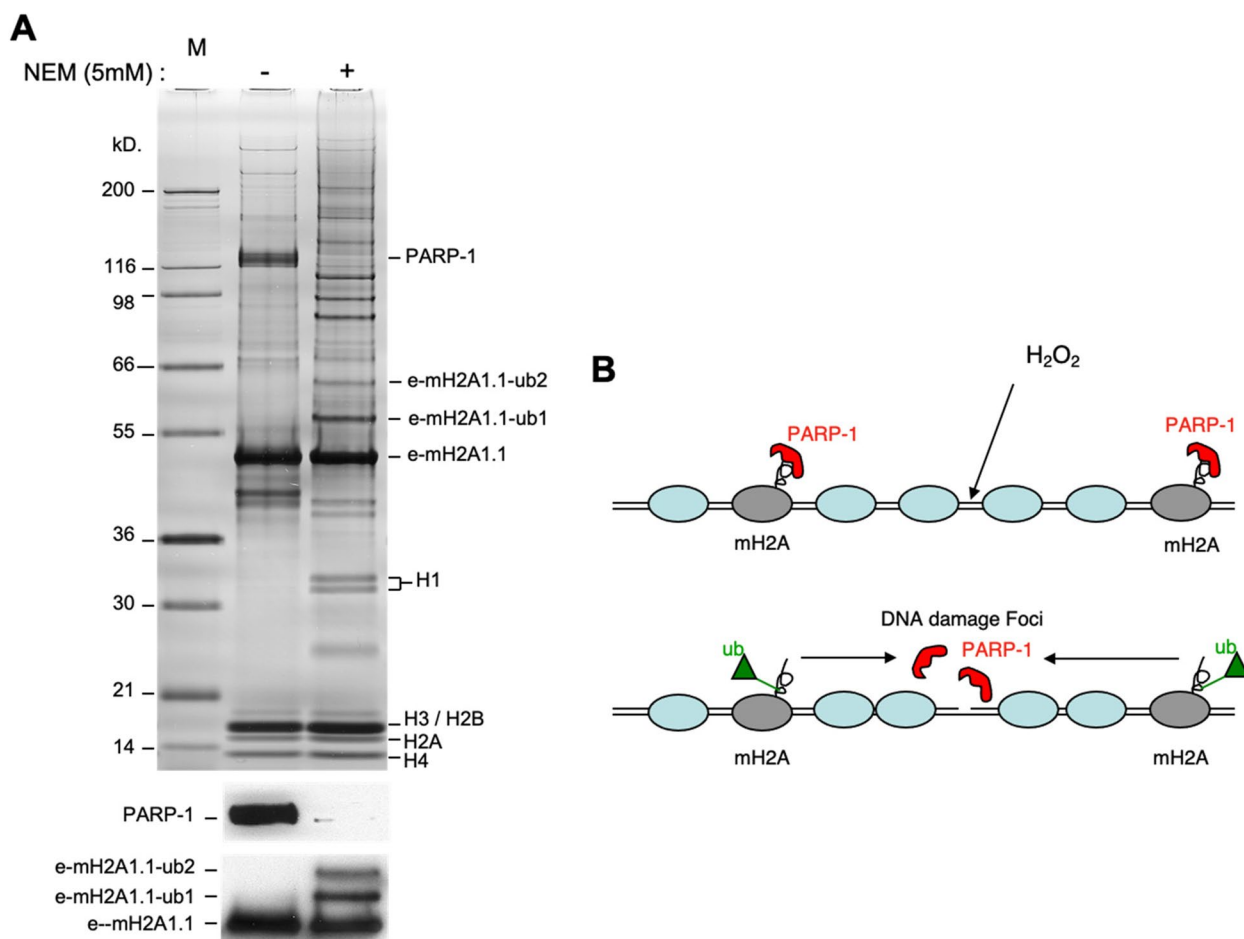


**Fig. 6** Ubiquitination of mH2A is sufficient to release PARP-1 from mH2A chromatin. **A** Treatment with NEM of stable HeLa cell lines expressing mH2A1.1 results in ubiquitination of mH2A1.1 and release of PARP-1 from the mH2A1 nucleosomal complex. Stable HeLa cell lines expressing mH2A1.1 were treated with 5 mM NEM for 30 min and mH2A1.1 nucleosomal complex was purified and run on a SDS PAGE. The protein bands were identified by mass spectrometry. The positions of PARP-1, non-modified and mono- and bi-ubiquitinated e-mH2A1.1 as well as histone H1 and the core histones are indicated. The Western blot of the respective e-mH2A1.1 complexes is shown in the lower part of the gel. The blot was first probed with anti-PARP-1 antibody and then, to visualize e-mH2A1.1, it was probed with anti-HA antibody. **B** Schematic presentation of the mechanism of PARP-1 release from the mH2A chromatin upon treatment with H<sub>2</sub>O<sub>2</sub>

a strongly activated and long-lived PARP-1 ([24] and this work). Importantly, no release of PARP-1 was detected when the cells were treated with either the DNA alkylating agents MMS or doxorubicin. These data show that: (i) mH2A1 is involved in DNA oxidative damage repair, (ii) this involvement is specific and, (iii) it is mediated through PARP-1.

Next, we have focused on the mechanism of PARP-1 release from mH2A1 nucleosomes upon oxidative stress. We hypothesized that the release of PARP-1 would be determined either by a direct effect of H<sub>2</sub>O<sub>2</sub> on structure of the mH2A1 nucleosome complex (for example, by inducing structural alterations in mH2A1 through direct interactions with OH<sup>•</sup>) or indirectly, by activating a specific pathway leading to posttranslational modification(s) in mH2A1. Since treatment of isolated mH2A1 nucleosomal complexes with H<sub>2</sub>O<sub>2</sub> showed no dissociation of PARP-1 from the nucleosomes, the hypothesis for a direct effect was rejected. We then investigated the modifications of mH2A1 induced after oxidative damage. We found that, in agreement with the available data [42], a modest amount of mH2A1 was mono-ubiquitinated in control cells. Oxidative damage resulted in both a strong increase of the amount of mono-ubiquitinated mH2A1 and the presence of bi-ubiquitinated mH2A1. The time course of mH2A1 ubiquitination was concomitant with the PARP-1 release from mH2A1 chromatin, suggesting that ubiquitination of mH2A1 would be implicated in the mechanism of PARP-1 release. In agreement with this, we found that mutations in the ubiquitinable mH2A1 lysine residues to alanines and thus, the creation of non-ubiquitinable mH2A1 mutants, interfered with the *in vivo* H<sub>2</sub>O<sub>2</sub>-induced release of PARP-1 and cell survival. Subsequent experiments showed that the *in vivo* generation of mH2A1 hyper-ubiquitination led to a quantitative release of PARP-1 from mH2A1 chromatin. It is important to note that the ubiquitination sites lie outside the mH2A1 macrodomain, which is responsible for PARP-1 binding, and hence their mutations cannot affect PARP-1 binding. The dissociation of PARP-1 from mH2A1 is very likely regulated by an off-rate that is influenced by the ubiquitination status of mH2A1. In instances where ubiquitination is absent, the dissociation of PARP-1 from mH2A1 still occurs but with a much slower kinetics, as observed in ubiquitination mutants (Fig. 5).

Interestingly, the e-mH2A1.1 nucleosome complexes, which were associated with PARP-1, were severely depleted of the linker histone H1, illustrating that the mutual binding of PARP-1 and H1 to chromatin was mutually exclusive, a result in agreement with the available data [43]. The ubiquitination of e-mH2A1 and the subsequent release of PARP-1 from chromatin

allowed the *de novo* binding of histone H1 to the mH2A chromatin.

Available data suggest that PARP-1 was associated with DNA and not with the macrodomain of mH2A1 within the e-mH2A1 nucleosomal complex [44]. Although, both *in vivo* treatment of the cells with H<sub>2</sub>O<sub>2</sub> (Fig. 2) and ubiquitination of the macrodomain of mH2A1 (Fig. 6) resulted in complete release of PARP-1 from the mH2A1 nucleosomal complex and consequently, these data do not support the above cited suggestion.

Since mH2A was related to the control of transcription, a possibility exists that the involvement of mH2A1 in DNA oxidative damage repair described here could be an indirect effect related to the function of mH2A1 in transcriptional regulation. However, we note that the transcription of genes related to DNA repair were not found to be affected in mH2A1 knockout mice [45] and no mH2A1 was found localized on the regulatory regions of DNA repair genes [24, 26], which rules out the above mentioned possibility.

We propose the following model for the role of mH2A in DNA oxidative repair (Fig. 6B). The interaction of PARP-1 with mH2A1 nucleosomes through the NHR of mH2A1 resulted in immobilization of the enzyme and downregulation of its catalytic activity [24] and this manuscript). Upon induction of oxidative damage, a ubiquitin ligase (responsible for the ubiquitination of mH2A) ubiquitinates mH2A resulting in the release of PARP-1 from the mH2A1 nucleosome complex. The released PARP-1 is then recruited to the sites of damage, where it is activated. The recruited PARP-1 organizes the repair of the damage by signaling the damage through poly(ADP-ribosylation) of some of the proteins involved in the repair, and also local decondensation of chromatin. Once the repair is completed, the PAR, which is synthesized and attached to the proteins, is degraded by PARG. PARP-1 is then recruited to the mH2A1 nucleosomes, and its enzymatic activity is again down regulated. In the absence of mH2A1, no efficient down regulation of the PARP-1 activity can be achieved, and active PARP-1 would remain present. In agreement with this, we found that the knock down of mH2A1 resulted in long lived activated PARP-1 in cells treated with H<sub>2</sub>O<sub>2</sub>, which, in turn, provokes the persistence of a high levels of poly(ADP-ribosylation) at the damage sites. The presence of PAR at levels above that required for proper repair, may interfere with its removal by the available PARG. This could result in the accumulation of long-lived PAR foci in the damaged cells, exactly as we have observed. In other words, the lack of mH2A1 in the cell would deregulate the very sophisticated mechanism of repair achieved by the concerted action of PARP-1 and PARG. Therefore, the role of

mH2A1 as a negative regulator of the PARP-1 enzymatic activity would be crucial for repair efficiency.

## Conclusions

This work demonstrated a direct link between mH2A1 and PARP-1 *in vivo*. PARP-1 is a multifunctional enzyme, which in addition to DNA repair and transcriptional regulation, is involved in several physiological processes, including cell division, DNA integrity, the balance between cell life versus death under physiological conditions, etc. [35, 37]. The direct link between mH2A1 and PARP-1 is also suggestive of an involvement of mH2A1 in these vital cellular processes. Whether mH2A1 plays a role in all these processes by regulating PARP-1 enzymatic activity remains a challenge for future studies.

## Methods

### Cell culture and transfection

HeLa cells were grown at 37°C in Dulbecco's modified Eagle's medium (Biowhitaker, Europe). Medium was supplemented with 10% foetal bovine serum (Biowhitaker, Europe). siRNA duplexes were introduced using Oligofectamine reagent (Invitrogen). To increase the suppression of mH2A1 mRNA, a double siRNA transfection was performed. Cells were recuperated 48h after the second transfection. The target sequences used (located in the NHR of mH2A1) were 5'-AAGCAGGGUGAAGUCAGUAAG-3' or 5'-ACAACCGAGGGCACACCUGCC-3' and the scrambled control sequence used was 5'-CAUGUCAUGUUCACAUCUCTT-3'.

### Generation of siRNA resistant mH2A1.1 cell line

RNAi-resistant mH2A1.1 construct was generated by creating silent point mutations in the cDNA. Briefly, the mH2A1.1 NHR region was changed from the original 5'-AAGCAGGGTGAAGTCAGTAAGGCA-3' to 5'-AAACAAGGAGAGGTAAGCAAAGCT-3'. The mutated mH2A1.1 sequence (sr\_mH2A1.1) was used to establish HeLa cells stably expressing a non-tagged siRNA-resistant mutant. The endogenous mH2A1 mRNA was knocked down using the following siRNA: 5'-AAGCAGGGUGAAGUCAGUAAG-3'.

### Treatment of HeLa cells with N-ethylmaleimide (NEM).

HeLa cells stably expressing e-mH2A1.1 were grown at 37°C in Dulbecco's modified Eagle's medium (Biowhitaker, Europe) and treated for 30 min with 5 mM NEM (Sigma). Treated cells were immediately collected and washed in PBS containing 1 mM NEM. The isolated nuclei were used for the purification of the e-mH2A1.1 nucleosome complexes.

### Purification of e-mH2A1.1 complexes

Stable cell lines expressing mH2A1.1 fused to its N-terminus with double-HA and double-FLAG epitope tags (e-mH2A1.1) was described in [24]. The isolated nuclei were digested with micrococcal nuclease to give predominantly mononucleosomes and the e-mH2A1.1 nucleosome complexes were prepared by immunopurification on anti-FLAG antibody conjugated agarose and/or anti-HA antibody conjugated agarose, respectively [24].

Lysine to alanine substitutions of the ubiquitination sites of e-mH2A1.1 were carried out by using standard mutagenesis techniques. The mutated e-mH2A1.1 nucleosomal complex was purified as described above for the wild type complex.

### Mass spectrometry

Identification of proteins was carried out using an Orbitrap mass spectrometer (ThermoFinnigan) by Taplin Biological Mass Spectrometry Facility (Harvard Medical School, Boston, MA).

### In vitro treatment of the e-mH2A1.1 nucleosome complexes

After micrococcal nuclease digestion of the nuclei, the e-mH2A1.1 nucleosome complexes were immobilized on an anti-FLAG antibody column and treated for 15 min with either 10 mM H<sub>2</sub>O<sub>2</sub> or 0.4 μM MMS or 20 mM doxorubicin at 4 °C. The attached to the resin complexes were washed three times with 10 volumes of 20 mM Tris-Cl pH 7.8, 150 mM NaCl, 1 mM EDTA (Ethylenediaminetetraacetic acid), 10% glycerol and analyzed on a 4–12% SDS-PAGE.

### Antibodies

Antibodies employed were as follows: monoclonal anti-Flag antibody M2 (Sigma), monoclonal anti-HA antibody 9E (Roche), monoclonal anti-PARP-1 ALX-804-211 (Enzo Life Sciences), monoclonal anti-ADP-ribose ALX-804-220 (Enzo Life Sciences), polyclonal anti-mH2A1 (Stefan Dimitrov, INSERM, Grenoble, France), polyclonal anti-mH2A1 ab37264 (Abcam), and polyclonal anti-H2A ab18975 (Abcam), anti-Ubiquitin mouse mAb (FK2) ST1200 (Sigma), Anti-Mouse IgG A6531 (Sigma).

### Immunofluorescence and Western Blot analysis and cell viability measurements

Western blot analysis and immunofluorescence were carried out as previously described [26]. For cell viability measurements, HeLa cells, transfected or not by siRNA against macroH2A1, were treated with different concentrations either with H<sub>2</sub>O<sub>2</sub> for 5 minutes at 4°C. Then the cells were rinsed twice with PBS and left to recover at 37°C. The viability of the cells was estimated 24h later by trypan blue counting.

### Comet assay

HeLa cells expressing or not siRNA resistant mH2A1.1, transfected or not with siRNA against macroH2A, were treated with 10mM H<sub>2</sub>O<sub>2</sub> for 5 minutes at 4°C, rinsed once with PBS and left to recover at 37°C for 0, 4, 8, 16, 20 and 60 minutes (to note is that we have used a relatively high concentration of H<sub>2</sub>O<sub>2</sub> (10mM) because of both the very short H<sub>2</sub>O<sub>2</sub> treatment (5 minutes) at low temperature (4°C) and the high resistance of the HeLa cells to H<sub>2</sub>O<sub>2</sub> induced damage; under our conditions 10 mM H<sub>2</sub>O<sub>2</sub> affects insignificantly cell viability, see Fig. 3). Then, the cells were immediately harvested and resuspended in cold PBS. 30 µl of the cell suspension was mixed with 270 µl of 0.6% low-melting agarose in PBS at 37 °C. Subsequently, 100 µl of the mixture were layered onto a slide pre-coated with thin layers of 1% agarose. The slides were left for 10 min on ice and were immediately immersed in cold lysis solution (2.5 M NaCl, 100 mM EDTA, 10 mM Tris, 1% sodium lauryl sarcosinate, 1% Triton 100 X and 10% DMSO, pH 10). After 1 h in the dark at 4 °C, the slides were immersed in alkaline electrophoresis buffer (1,2% NaOH, 1 mM EDTA) for unwinding (30 min) and then submitted to electrophoresis (25 V/300 mA, 40 min). Once the electrophoresis was completed, the slides were neutralized (3×5 min; 0.4 M Tris pH 7.5). The slides were stained with ethidium bromide prior to analysis with a Zeiss fluorescence microscope. The microscope was connected to a charge-coupled device (CCD) camera and a computer-based analysis system (comet Analysis Software, version 3.1, Kinetic Imaging Limited). The results were expressed as percentage of DNA in the tail (% Tail DNA).

### Poly ADPribose (PAR) detection

HeLa cells, transfected or not by siRNA and/or pCDNA vector, were treated with 10 mM H<sub>2</sub>O<sub>2</sub> for 5 minutes at 4°C, rinsed once with PBS and left to recover at 37°C for 4, 8, 15, 20, 25, 30 and 35 minutes, respectively. The cells were then immediately either (i) harvested and assayed for poly(ADP-ribose) formation by Western Blot or, (ii) fixed for immunofluorescence. The PAR foci were visualized with the anti-poly (ADP-ribose) antibody and number of positive nuclei for ADP-ribose foci was estimated. No less than 100 cells were analyzed in each experiment.

### Abbreviations

PARP-1	Poly(ADP-ribose) polymerase I
PAR	Poly(ADP-ribose)
PARG	Poly(ADP-ribose) glycohydrolase
mH2A	MacroH2A
NHR	Non-Histone Region
NAD	Nicotinamide adenine dinucleotide
MMS	Methyl methanesulfonate
NEM	N-ethylmaleimide
SSB	Single strand breaks
Xi	Inactive X chromosome (Xi)
SDS	Sodium dodecyl sulfate
PAGE	Polyacrylamide gel
EDTA	Ethylenediaminetetraacetic acid

### Supplementary Information

The online version contains supplementary material available at <https://doi.org/10.1186/s12915-024-01987-x>.

**Additional file 1: Fig. S1.** MMS or doxorubicin treatment of stable HeLa cell lines expressing e-mH2A1.1 did not result in a release of PARP-1 from the e-mH2A1.1 nucleosome complex. **(A)** e-mH2A1.1 nucleosome complexes were purified from either control, or MMS or doxorubicin treated stable HeLa cell lines expressing e-mH2A1.1. A single immunopurification step of the e-mH2A1.1 complex through a column containing covalently attached anti-FLAG antibodies was used. The positions of the bands corresponding to PARP-1 and e-mH2A1.1 are indicated. Lane M, protein molecular mass marker. **(B)** Western blot of e-mH2A1.1 nucleosome complexes isolated from either control, or MMS or doxorubicin treated e-mH2A1.1 stable HeLa cell lines. The blot was first revealed with anti-PARP-1 antibody and then, to visualize e-mH2A1.1, it was revealed with anti-HA antibody. Note that upon treatment with either one of the DNA damaging agents no release of PARP-1 was detected.

**Additional file 2: Fig. S2.** H<sub>2</sub>O<sub>2</sub> treatment of isolated e-mH2A1.1 nucleosome complexes did not lead to dissociation of PARP-1 from the nucleosome complexes. **(A)** e-mH2A1.1 nucleosome complexes (isolated by a single immunopurification step from stable HeLa cell lines expressing e-mH2A1.1) were either non-treated (Ctrl) or treated with either H<sub>2</sub>O<sub>2</sub>, or MMS or doxorubicin and were separated on SDS PAGE. The gel was silver stained. The positions of PARP-1 and e-mH2A1.1 are indicated. M, molecular mass marker. **(B)** Western blot analysis of e-mH2A1.1 nucleosome complexes treated with H<sub>2</sub>O<sub>2</sub>, MMS and doxorubicin. e-mH2A1.1 nucleosome complexes were isolated from HeLa cells and then treated with either H<sub>2</sub>O<sub>2</sub> or MMS or doxorubicin. After separation on SDS-PAGE, the proteins from the complexes were transferred to a nitrocellulose membrane and were first probed with anti-PARP-1 antibody and then, to visualize e-mH2A1.1, the blot was probed with anti-HA antibody. Note that treatment of the isolated mH2A1.1 nucleosomal complexes with either one of the damaging agents did not lead to dissociation of PARP-1 from the mH2A1.1 nucleosomes.

### Acknowledgements

We thank S. Sauvaigo for advices in the Comet assay experiments and D. Angelov, L. for critical reading of the manuscript. This research work was funded by Institutional Fund Project under grant number (IFPNC-005-130-2020). Authors therefore gratefully acknowledge technical support from Ministry of Education and King Abdulaziz University, Jeddah, Saudi Arabia.

### Authors' contributions

Conceptualization, AH and SD; Formal analysis, KO, FM, JSMS, AM and AB; Funding acquisition, AH and SD; Investigation, KO, FM, JSMS, AM and AI, HM and CB; Methodology, KO, FM, AM, AI, RSA, ATZ and AB; Project administration, AH; Supervision, AH; Validation, FM; Visualization, KO and FM; Writing – original draft, AH and SD. All authors read and approved the final manuscript.

### Funding

This work was supported by institutional funds from CNRS, INSERM, Université de Strasbourg (UDS), the Labex INRT and by grants from Fondation pour la Recherche Médicale (FRM) (Equipe labellisée A.H.), Agence National pour la Recherche (ANR-21-CE12-0017 RAHMAN, ANR-21-CE11-0024 SIMOS, ANR-20-CE17-0008\_CA-Ts, ANR-18-CE12-0010\_ZFun). This research work was funded by the project 101 086 923 – AEGIS-IMB and by Institutional Fund Project from Ministry of Education and King Abdulaziz University, Jeddah, Saudi Arabia. Under grant number (IFPNC-005–130-2020).

### Availability of data and materials

All data supporting the findings of this study are available within the article and within its supplementary materials published online.

### Declarations

### Ethics approval and consent to participate

Not applicable.

**Consent for publication**

Not applicable.

**Competing interests**

The authors declare that they have no competing interests.

Received: 20 August 2023 Accepted: 18 August 2024

Published online: 02 September 2024

**References**

- van Holde K. Chromatin. Berlin: Springer-Verlag KG; 1988.
- Lattrick CM, Marek M, Ouararhni K, Papin C, Stoll I, Ignatyeva M, Obri A, Ennifar E, Dimitrov S, Romier C, et al. Molecular basis and specificity of H2A.Z-H2B recognition and deposition by the histone chaperone YL1. *Nat Struct Mol Biol.* 2016;23(4):309–16.
- Obri A, Ouararhni K, Papin C, Diebold ML, Padmanabhan K, Marek M, Stoll I, Roy L, Reilly PT, Mak TW, et al. ANP32E is a histone chaperone that removes H2A.Z from chromatin. *Nature.* 2014;505(7485):648–53.
- Drane P, Ouararhni K, Depaux A, Shuaib M, Hamiche A. The death-associated protein DAXX is a novel histone chaperone involved in the replication-independent deposition of H3.3. *Genes Dev.* 2010;24(12):1253–65.
- Shuaib M, Ouararhni K, Dimitrov S, Hamiche A. HJURP binds CENP-A via a highly conserved N-terminal domain and mediates its deposition at centromeres. *Proc Natl Acad Sci U S A.* 2010;107(4):1349–54.
- Doyen CM, An W, Angelov D, Bondarenko V, Miettton F, Studitsky VM, Hamiche A, Roeder RG, Bouvet P, Dimitrov S. Mechanism of polymerase II transcription repression by the histone variant macroH2A. *Mol Cell Biol.* 2006;26(3):1156–64.
- Bao Y, Konesky K, Park YJ, Rosu S, Dyer PN, Rangasamy D, Tremethick DJ, Laybourn PJ, Luger K. Nucleosomes containing the histone variant H2A.Bbd organize only 118 base pairs of DNA. *EMBO J.* 2004;23(16):3314–24.
- Doyen CM, Montel F, Gautier T, Menoni H, Claudet C, Delacour-Larose M, Angelov D, Hamiche A, Bednar J, Faivre-Moskalenko C, et al. Dissection of the unusual structural and functional properties of the variant H2A.Bbd nucleosome. *EMBO J.* 2006;25(18):4234–44.
- Angelov D, Verdel A, An W, Bondarenko V, Hans F, Doyen CM, Studitsky VM, Hamiche A, Roeder RG, Bouvet P, et al. SWI/SNF remodeling and p300-dependent transcription of histone variant H2A.Bbd nucleosomal arrays. *EMBO J.* 2004;23(19):3815–24.
- Roulland Y, Ouararhni K, Naidenov M, Ramos L, Shuaib M, Syed SH, Lone IN, Boopathi R, Fontaine E, Papai G et al. The flexible ends of CENP-A Nucleosome are required for mitotic fidelity. *Mol Cell.* 2016;18(63(4):674–85.
- Shukla MS, Syed SH, Montel F, Faivre-Moskalenko C, Bednar J, Travers A, Angelov D, Dimitrov S. Remosomes: RSC generated non-mobilized particles with approximately 180 bp DNA loosely associated with the histone octamer. *Proc Natl Acad Sci U S A.* 2010;107(5):1936–41.
- Shukla MS, Syed SH, Goutte-Gattat D, Richard JL, Montel F, Hamiche A, Travers A, Faivre-Moskalenko C, Bednar J, Hayes JJ, et al. The docking domain of histone H2A is required for H1 binding and RSC-mediated nucleosome remodeling. *Nucleic Acids Res.* 2011;39(7):2559–70.
- Menoni H, Shukla MS, Gerson V, Dimitrov S, Angelov D. Base excision repair of 8-oxoG in dinucleosomes. *Nucleic Acids Res.* 2012;40(2):692–700.
- Angelov D, Molla A, Perche PY, Hans F, Cote J, Khochbin S, Bouvet P, Dimitrov S. The Histone Variant MacroH2A Interferes with Transcription Factor Binding and SWI/SNF Nucleosome Remodeling. *Mol Cell.* 2003;11(4):1033–41.
- Ryan DP, Tremethick DJ. The interplay between H2A.Z and H3K9 methylation in regulating HP1 $\alpha$  binding to linker histone-containing chromatin. *Nucleic Acids Res.* 2018;46(18):9353–66.
- Andronov L, Ouararhni K, Stoll I, Klaholz BP, Hamiche A. CENP-A nucleosome clusters form rosette-like structures around HJURP during G1. *Nat Commun.* 2019;10(1):4436.
- Sarma K, Reinberg D. Histone variants meet their match. *Nat Rev Mol Cell Biol.* 2005;6(2):139–49.
- Pehrson JR, Fried VA. MacroH2A, a core histone containing a large nonhistone region. *Science.* 1992;257:1398–400.
- Pehrson J, Fujii RN. Evolutionary conservation of histone macroH2A subtypes and domains. *Nucl Acids Res.* 1998;26:2837–42.
- Chadwick BP, Valley CM, Willard HF. Histone variant macroH2A contains two distinct macrochromatin domains capable of directing macroH2A to the inactive X chromosome. *Nucleic Acids Res.* 2001;29:2699–705.
- Sun Z, Bernstein E. Histone variant macroH2A: from chromatin deposition to molecular function. *Essays Biochem.* 2019;63(1):59–74.
- Hurtado-Bages S, Guberovic I, Buschbeck M. The MacroH2A1.1 - PARP1 Axis at the Intersection Between Stress Response and Metabolism. *Front Genet.* 2018;9:417.
- Agelopoulos M, Thanos D. Epigenetic determination of a cell-specific gene expression program by ATF-2 and the histone variant macroH2A. *EMBO J.* 2006;25(20):4843–53.
- Ouararhni K, Hadj-Slimane R, Ait-Si-Ali S, Robin P, Miettton F, Harel-Bellan A, Dimitrov S, Hamiche A. The histone variant mH2A1.1 interferes with transcription by down-regulating PARP-1 enzymatic activity. *Genes Dev.* 2006;20(23):3324–36.
- Costanzi C, Pehrson JR. Histone macroH2A1 is concentrated in the inactive X chromosome of female mammals. *Nature.* 1998;393:599–601.
- Miettton F, Sengupta AK, Molla A, Picchi G, Barral S, Heliot L, Grange T, Wutz A, Dimitrov S. Weak but uniform enrichment of the histone variant macroH2A1 along the inactive X chromosome. *Mol Cell Biol.* 2009;29(1):150–6.
- Changolkar LN, Pehrson JR. macroH2A1 histone variants are depleted on active genes but concentrated on the inactive X chromosome. *Mol Cell Biol.* 2006;26(12):4410–20.
- Pliatska M, Kapasa M, Kokkalis A, Polyzos A, Thanos D. The Histone Variant MacroH2A Blocks Cellular Reprogramming by Inhibiting Mesenchymal-to-Epithelial Transition. *Mol Cell Biol.* 2018;38(10):e00669-e717.
- Hodge DQ, Cui J, Gamble MJ, Guo W. Histone Variant MacroH2A1 Plays an Isoform-Specific Role in Suppressing Epithelial-Mesenchymal Transition. *Sci Rep.* 2018;8(1):841.
- Kim J, Sun C, Tran AD, Chin PJ, Ruiz PD, Wang K, Gibbons RJ, Gamble MJ, Liu Y, Oberdoerffer P. The macroH2A1.2 histone variant links ATRX loss to alternative telomere lengthening. *Nat Struct Mol Biol.* 2019;26(3):213–9.
- Posavec Marjanovic M, Hurtado-Bages S, Lassi M, Valero V, Malinverni R, Delage H, Navarro M, Corujo D, Guberovic I, Douet J, et al. MacroH2A1.1 regulates mitochondrial respiration by limiting nuclear NAD(+) consumption. *Nat Struct Mol Biol.* 2017;24(11):902–10.
- Khurana S, Kruhlak MJ, Kim J, Tran AD, Liu J, Nyswaner K, Shi L, Jailwala P, Sung MH, Hakim O, et al. A macrohistone variant links dynamic chromatin compaction to BRCA1-dependent genome maintenance. *Cell Rep.* 2014;8(4):1049–62.
- Kozlowski M, Corujo D, Hothorn M, Guberovic I, Mandemaker IK, Blessing C, Sporn J, Gutierrez-Triana A, Smith R, Portmann T, et al. MacroH2A histone variants limit chromatin plasticity through two distinct mechanisms. *EMBO Rep.* 2018;19(10):e44445.
- Cadet J, Ravanat JL, Martinez GR, Medeiros MH, Di Mascio P. Singlet oxygen oxidation of isolated and cellular DNA: product formation and mechanistic insights. *Photochem Photobiol.* 2006;82(5):1219–25.
- Schreiber V, Dantzer F, Ame JC, de Murcia G. Poly(ADP-ribose): novel functions for an old molecule. *Nat Rev Mol Cell Biol.* 2006;7(7):517–28.
- Poirier GG, de Murcia G, Jongstra-Bilen J, Niedergang C, Mandel P. Poly(ADP-ribose)ylation of polynucleosomes causes relaxation of chromatin structure. *Proc Natl Acad Sci U S A.* 1982;79(11):3423–7.
- Kim MY, Zhang T, Kraus WL. Poly(ADP-ribose)ylation by PARP-1: “PAR-laying” NAD<sup>+</sup> into a nuclear signal. *Genes Dev.* 2005;19(17):1951–67.
- Okano S, Lan L, Caldecott KW, Mori T, Yasui A. Spatial and temporal cellular responses to single-strand breaks in human cells. *Mol Cell Biol.* 2003;23(11):3974–81.
- Nusinow DA, Hernandez-Munoz I, Fazio TG, Shah GM, Kraus WL, Panning B. Poly(ADP-ribose) polymerase 1 is inhibited by a histone H2A variant, MacroH2A, and contributes to silencing of the inactive X chromosome. *J Biol Chem.* 2007;282(17):12851–9.
- D’Amours D, Desnoyers S, D’Silva I, Poirier GG. Poly(ADP-ribose)ylation reactions in the regulation of nuclear functions. *Biochem J.* 1999;342(Pt 2):249–68.
- Nakajima H, Nagaso H, Kakui N, Ishikawa M, Hiranuma T, Hoshiko S. Critical role of the automodification of poly(ADP-ribose) polymerase-1 in nuclear factor-kappaB-dependent gene expression in primary cultured mouse glial cells. *J Biol Chem.* 2004;279(41):42774–86.
- Abbott DW, Chadwick BP, Thambirajah AA, Ausio J. Beyond the Xi: macroH2A chromatin distribution and post-translational modification in an avian system. *J Biol Chem.* 2005;280(16):16437–45.

43. Krishnakumar R, Gamble MJ, Frizzell KM, Berrocal JG, Kininis M, Kraus WL. Reciprocal binding of PARP-1 and histone H1 at promoters specifies transcriptional outcomes. *Science*. 2008;319(5864):819–21.
44. Timinszky G, Till S, Hassa PO, Hothorn M, Kustatscher G, Nijmeijer B, Colombelli J, Altmeyer M, Stelzer EH, Scheffzek K, et al. A macrodomain-containing histone rearranges chromatin upon sensing PARP1 activation. *Nat Struct Mol Biol*. 2009;16(9):923–9.
45. McKeown K, Changolkar L, Pehrson J, editors. Utilizing cDNA subtraction to examine the effects of mH2A deletion in a colony of knockout female mice. 2006 MERCK/MERIAL National Veterinary Scholar Symposium: Creating the gumbo of progress; School of Veterinary Medicine, Louisiana State University. Baton Rouge; 2006. p. 146.

### **Publisher's Note**

Springer Nature remains neutral with regard to jurisdictional claims in published maps and institutional affiliations.